IEEE Access
Multidisciplinary | Rapid Review | Open Access Journal

Received 31 August 2022, accepted 16 October 2022, date of publication 21 October 2022, date of current version 28 October 2022.

Digital Object Identifier 10.1109/ACCESS.2022.3216237

RESEARCH ARTICLE

A Reconfigurable Metal Rim Antenna With Smallest Clearance for Smartphone Applications

LYUWEI CHEN[1], YI HUANG[1], (Fellow, IEEE), HANYANG WANG[2], (Fellow, IEEE), HAI ZHOU[2], AND KEXIN LIU[3]

[1]Department of Electrical Engineering and Electronics, University of Liverpool, L69 3GJ Liverpool, U.K.
[2]Huawei Technology (U.K.) Company Ltd., RG2 6AD Reading, U.K.
[3]Huawei Technology Company Ltd., Shanghai 518129, China

Corresponding author: Yi Huang (Yi.Huang@Liverpool.ac.uk)

This work was supported in part by the University of Liverpool, and in part by Huawei Technology.

ABSTRACT In this paper, a reconfigurable metal rim antenna with a small clearance and compact structure for 4G/5G smartphones is proposed. It consists of the system ground plane and a metal rim with two slits, in which a U-shaped slot of 1 mm (the smallest) clearance is realized between the system ground and metal rim. The theory of characteristic modes is applied to analyze the eigenmodes of the antenna so as to aid the optimum design. The characteristic modes (CMs) in the band of interest are studied, and an inductive coupling exciter is identified as the best since three CMs can therefore be generated in the lower frequency band (0.69-0.96 GHz), and an SP4T switch can be utilized to increase the bandwidth of the whole lower band. A prototype antenna of the optimized design was fabricated. A good agreement was obtained between the measured and simulated results. The 6-dB frequency bands are the lower band (0.69-0.96 GHz), the middle band (1.7- 2.7 GHz), and the higher 5G band (3.4- 3.6 GHz), respectively, and the total efficiencies are over 50% in all these frequency bands. They indicate that the antenna is a very good candidate for smartphone applications.

INDEX TERMS Metal rim antenna, mobile antenna, reconfigurable antenna, small ground clearance, theory of characteristic modes.

I. INTRODUCTION

With the rapid development of wireless communication technology [1], users are increasingly demanding high-end smartphones with many flagship features. Since the space available for antennas is very limited in a smartphone, the all-metal rim antenna with a high screen ratio, high data rates, and gorgeous appearance, covers the 2G/3G/4G bands (0.69 – 0.96 GHz and 1.7 – 2.7 GHz) and 5G band (3.4- 3.6 GHz) are very attractive and competitive. However, the emergence of 5G antennas has reduced the available space of the 4G antennas. Besides, with the trend towards a larger high screen-to-body ratio, the ground clearance referring to the no-ground portion of the terminal becomes smaller. Therefore, designing a metal rim antenna for 4G/5G bands with a small clearance between the metal rim and the ground plane is extremely challenging and attractive.

Many interesting designs of meal rim antennas have been developed by researchers. To obtain a good bandwidth and efficiency, one common method is to transform the metal rim into an antenna radiator. The metal frame can be divided into two categories: one is the entire metal rim as the antenna radiator [2], [3], [4], [5], [6], [7], and the other is a part of the metal rim as the antenna radiator [8], [9], [10], [11], [12], [13], [14], [15], [16], [17], [18]. In [2], the whole metal frame was used as a radiator without any other antenna elements, and an inductive coupling feeding source was employed to cover the lower band from 0.8 GHz to 1.0 GHz and the middle band from 1.7 GHz to 2.7 GHz, respectively. But this design retained a large ground clearance of 15 mm between the system ground plane and the metal frame. In contrast, the designs in [8], [9], [10], [11], [12], [13], [14], [15], [16], [17],

The associate editor coordinating the review of this manuscript and approving it for publication was Debabrata Karmokar.

and [18] have utilized other techniques to design smartphone antennas, such as loading lump elements [8], [9], [10], [14], parasitic branches [10], [11], [15], [17], or distributed element matching networks [12], [13], [16] into the clearance area to obtain multi-band or wide broadband operation. In [9], an L-shaped microstrip line was used as a capacitive coupling feeding source to cover the lower band with a ground clearance of 5 mm, while an L-shaped grounded branch was employed to increase the bandwidth of the higher band. In [12], [13], and [16], the proposed antennas can cover the lower band (0.76-0.96 GHz) and middle band (1.7-2.7 GHz) without any matching work. However, these methods need a large clearance. It's not suitable for full-screen smartphones nowadays.

However, these designs do not cover the new 5G band (e.g., 3.4 – 3.6 GHz). There are some metal rim antenna designs for 5G smartphones, but most of them cannot cover the 4G and 5G bands (0.69-0.96 GHz, 1.7- 2.9 GHz, and 3.4- 3.6 GHz) simultaneously. The antenna in [19] can cover 4G/5G bands, but the ground clearance was 10 mm, which is too large to meet the antenna design requirement for the full-screen smartphone. It is extremely important to ensure the clearance is as small as possible in modern smartphone designs. Therefore, a metal rim antenna with the smallest clearance that can cover 4G/5G bands is in high demand and is also the main objective of this research.

To conduct a comprehensive and systematic study of the metal rim antenna so as to obtain the best design, the theory of characteristic modes (TCM) has been used, which was introduced by Harrington and Mautz in the 1970s [20], [21], and recently, it has received significant attention for the design of mobile phone antennas. TCM can provide a clear understanding of the physical behaviour of the antenna and is becoming an important method for analyzing the working mechanism of the antenna. Some metal rim antenna designs using TCM as a guideline for mobile terminal antennas have been reported in [10], [22], [23], and [24]. In [24], the characteristic mode (CM) of the metal rim has been analyzed for the lower band, and it indicates that the metal rim modes can be used to cover the bands below 1 GHz. Based on the TCM, a monopole antenna as a capacitive coupling exciter has been integrated into a full metal frame, while the higher band (1.7-2.7 GHz) is achieved by printed multiple branches, but the ground clearance is up to 11 mm. In [26], a lower band metal rim antenna based on the TCM was proposed, and the clearance was 2 mm, but it only covered 0.82-0.97 GHz. A further initial study was reported in [27], covering the working frequency of 0.85 to 0.96 GHz and 1.71-2.69 GHz. However, it does not cover the whole lower band (0.69-0.96 GHz) and the higher 5G band (3.4-3.6 GHz).

In this paper, a comprehensive study is presented, and a reconfigurable metal rim antenna with a small clearance for 4G/5G smartphones is proposed and studied by using the TCM. According to the current distributions of CMs, two slits are introduced at the upper part of the metal frame to get a new CM in the lower band. Then an inductive coupling

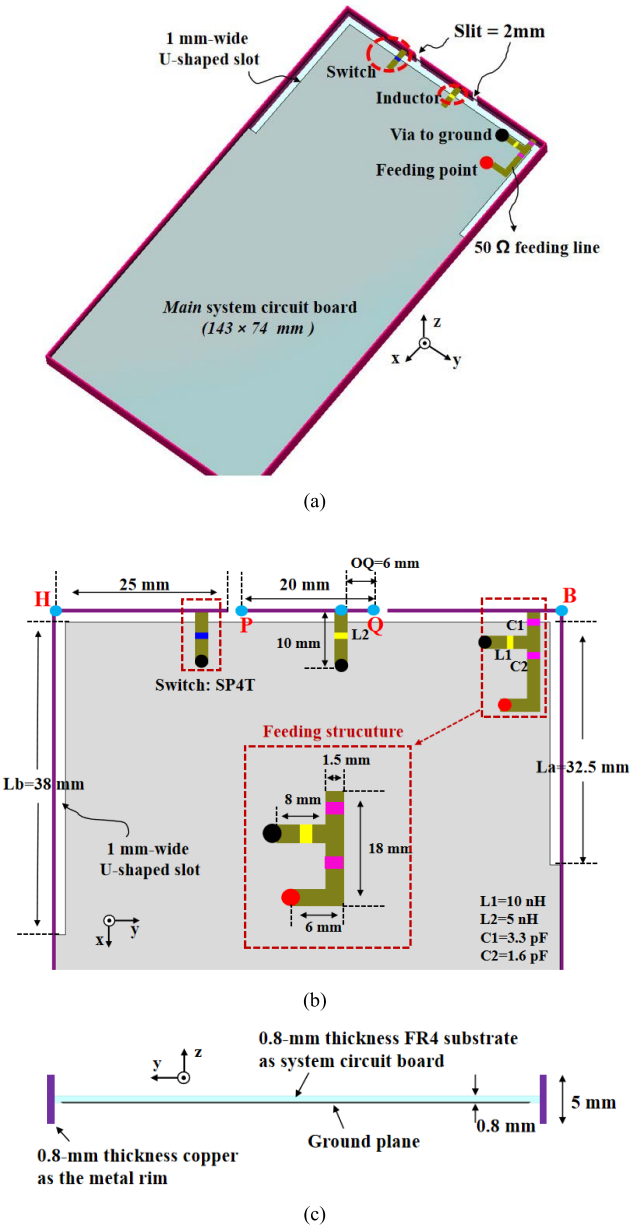

FIGURE 1. Proposed reconfigurable metal rim antenna configuration (a) 3D view of the metal rim antenna. (b) Detailed dimensions of the proposed antenna. (c) Cross-section view (from the middle).

exciter is used to excite three resonant CMs of the ground and metal rim. An SP4T switch is utilized to increase the bandwidth of the lower band (0.69 - 0.96 GHz). The ground clearance is only 1 mm between the metal rim and the system ground, the smallest in the literature. Therefore, the proposed metal rim antenna outperforms all other antennas and has the potential to be utilized in the popular high screen-to-body ratio smartphone applications.

II. DESIGN AND ANALYSIS OF THE PROPOSED ANTENNA

A. CONFIGURATION OF ANTENNA

Fig.1 shows the geometry of the proposed metal rim antenna. As shown in Fig. 1(a), an FR4 substrate with a thickness of

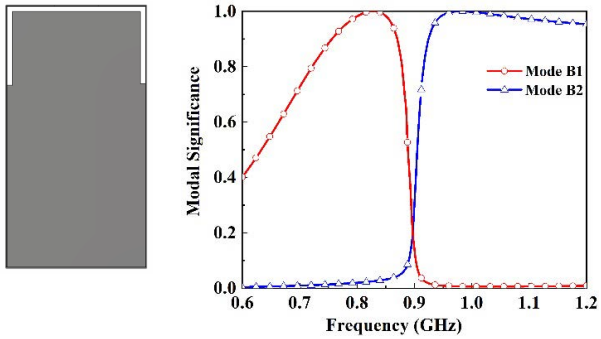

(a) (b)

FIGURE 2. (a) The simplified model (unbroken metal rim). (b) MS in the lower band.

0.8-mm, a dielectric constant of 4.4, and the loss tangent of 0.024 is served as a system printed circuit board (PCB) with a dimension of 143 × 74 mm^2. A metal frame surrounds the substrate with a thickness of 0.8 mm and a height of 5 mm. A major portion of the metal rim is shorted to the ground plane, thereby increasing the mechanical stability and keeping the compact size of the antenna. A 1 mm-wide U-shaped slot is located between the metal rim and the system ground, while two symmetrical slits with a width of 2 mm are opened at the upper part of the metal rim.

As illustrated in Fig. 1(b), the proposed reconfigurable meal rim antenna mainly contains a SP4T switch, a feeding network, and two slits at the upper part of the metal rim. A 50-Ω microstrip line is used to feed the metal rim directly. The matching circuit and the SP4T switch are shown in the dashed red box. The PCB is positioned at the centre of the metal rim, as shown in Fig. 1(c). The electromagnetic solvers, Altair FEKO and CST microwave studio (they have different strengths), are utilized for characteristic mode analysis (CMA), antenna design and parameter optimizations.

B. LOWER BAND ANALYSIS

In a narrow space surrounded by a floating metal frame, it is a huge challenge to cover the entire frequency band (2G/3G/4G/5G), especially in the lower band. The metal frame around the phone will significantly affect the antenna performance, such as bandwidth and radiation efficiency. Therefore, the TCM has drawn increased interest in mobile handset antenna design and has been employed to solve the above problems. The TCM brings clearer insights into the physical behaviour of an antenna by providing a framework for analyzing the antenna structure without any feeding structure. From the TCM, the characteristic modes of an antenna are only affected by its shape and material and are irrelevant to excitation. The detailed derivation of TCM and its application can be found in [20], [21], and [28].

CMs can be defined by

$$X(J_n) = \lambda_n R(J_n) \tag{1}$$

where λ_n is the eigenvalue associated with the n^{th} mode and J_n the eigenvector; R and X are the real and imaginary parts of the impedance matrix, respectively. The mode will be a resonant mode when λ_n is equal to 0.

The modal significance (MS) illustrates the ability of each CM coupling with an external source. It is independent of the external source and is an inherent property of the characteristic modes. It can be described in the following equation:

$$MS = \left| \frac{1}{1 + j\lambda_n} \right| \tag{2}$$

When the MS is more than $1/\sqrt{2}$, the mode is considered to be excited.

The current on a conductive surface excited by an exciter can be expressed as a linear superposition of the normalized eigencurrents as

$$J = \sum_1^n \alpha_n J_n \tag{3}$$

where α_n denotes the modal weighting coefficient (MWC) of the n^{th} CM. The magnitude of α_n presents the contribution of the corresponding mode to the total antenna surface current, and J_n represents its eigencurrent distribution. Where J is the sum of eigencurrents (J_n). Furthermore, α_n can be calculated as

$$\alpha_n = \frac{V_n^{ex}}{1 + j\lambda_n} \tag{4}$$

α_n is determined by the modal significance and the external excitation V_n^{ex}. Therefore, the feeding location of the source and excitation method is crucial to the antenna design.

Fig. 2(a) shows the 3-D view of the simplified model. An unbroken metal rim with the size of 143 × 74 × 5 mm^3 is used for our initial analysis, and the gap between the metal rim and the ground plane is 1 mm. The modal significances are shown in Fig. 2(b). It is shown that Modes B1 and B2 approach one at 0.84 GHz and 1.0 GHz, respectively. To analyze the operating principle of the two modes, the eigencurrents are shown in Fig. 3 at their respective resonant frequencies. It can be seen that strong currents are around the U-shaped slot in Fig. 3(a) and (b), identifying these as the slot modes. Two current zeros appear in the centre of the short side of the PCB and the metal frame. Therefore, Modes B1 and B2 are associated with the 1λ mode. It can also be observed that Modes B1 and B2 have very similar current distributions. The only difference is the current distribution at the lower part of the structure. For Mode B1, the current is in phase at points G and C, out of phase of the ground plane. But for Mode B2, the current is out of phase at points G and C, in phase on the ground plane. Therefore, only one resonance can be generated when excitation is introduced.

Because of the similar characteristics, the feeding source can be put at any place around the U-shaped slot. Here we choose to place it close to the maximum current point G, which means an inductive coupling feeding method is introduced [29]. The result can be obtained by using CMA as depicted in Fig. 4. The modal weighting coefficient (MWC) is an important parameter for evaluating whether a CM is effectively excited or not. As shown in Fig. 4(b), Mode B1

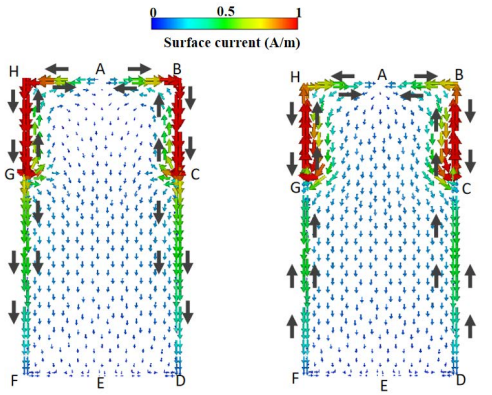

(a) (b)

FIGURE 3. Simulated eigencurrent distribution and normalized patterns of the metal rim configuration. (a) Mode B1 at 0.84 GHz. (b) Mode B2 at 1.0 GHz.

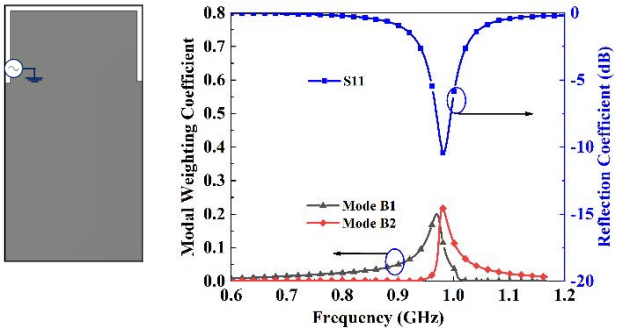

(a) (b)

FIGURE 4. (a) Configuration of the inductive exciter. (b) Magnitudes of MWC after adding the exciter and the reflection coefficient.

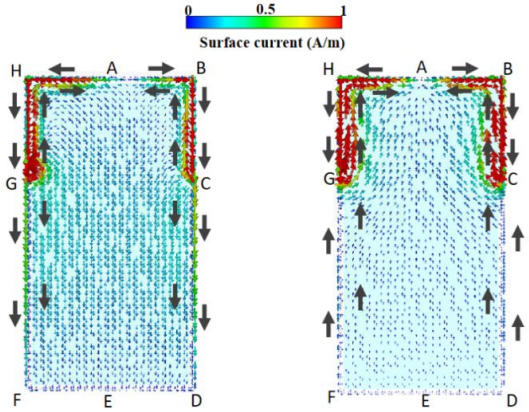

(a) (b)

FIGURE 5. Simulated total currents at 0.97 GHz. (a) Phase=0 degree. (b) Phase=90 degree.

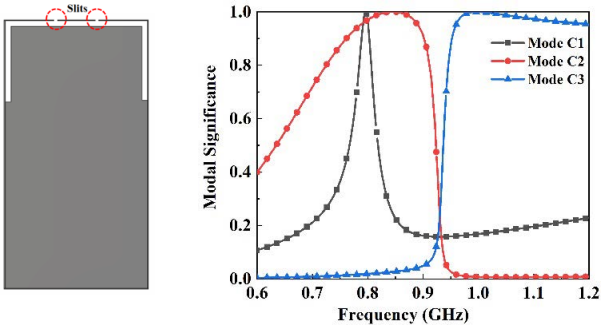

(a) (b)

FIGURE 6. (a) Modified configuration. (b) MS in the lower band.

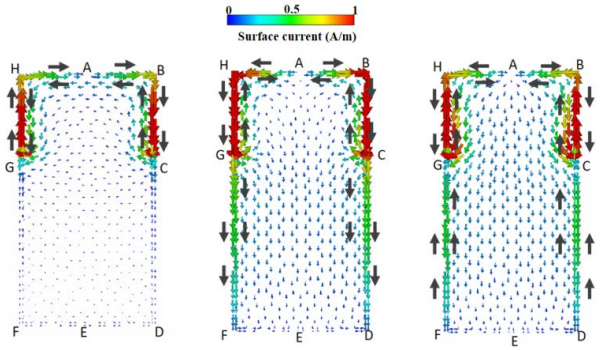

(a) (b) (c)

FIGURE 7. Simulated eigencurrents of the open two slits. (a) Mode C1 at 0.8 GHz. (b) Mode C2 at 0.84 GHz. (c) Mode C3 at 1.0 GHz.

and Mode B2 are excited simultaneously at 0.97 GHz with different MWC magnitudes, which validate the aforementioned prediction. The current distributions at different phases are shown in Fig. 5, and we can see that when the phase is 0 degree, it is similar to the eigencurrent Mode B1; when the phase is 90 degrees, it looks the same as the eigencurrent Mode B2. It can prove that Modes B1 and B2 are combined at one resonance. However, the 6-dB bandwidth is very narrow, only from 0.95 to 0.98 GHz, which does not meet the mobile terminal requirement.

To increase the bandwidth [26] of the lower band, as shown in Fig. 6(a), two slits at the minimum current position at the upper part of the metal frame without affecting Modes B1 and B2 are introduced. As shown in Fig. 6(b), a new Mode C1, regarded as an open slot mode, at 0.8 GHz is generated in the lower band. Modes C2 and C3 approach one at 0.84 GHz and 1.0 GHz, respectively, which are very similar to Modes B1 and B2. The eign-current distributions shown in Fig. 7 can also prove that. It can be easily found that Mode C1 has different characteristics from Modes C2 and C3. The current direction of Mode C1 is in phase around the U-shaped slot and is 0.5λ. The radiation pattern of Mode C1 is orthogonal to Modes C2 and C3, which can be utilized to design high isolation MIMO antennas.

Apparently, Modes C1, C2 and C3 have similar current distribution around the U-shaped slot. Therefore, an inductive coupling feeding source located at the maximum current position near point G is utilized to excite the three

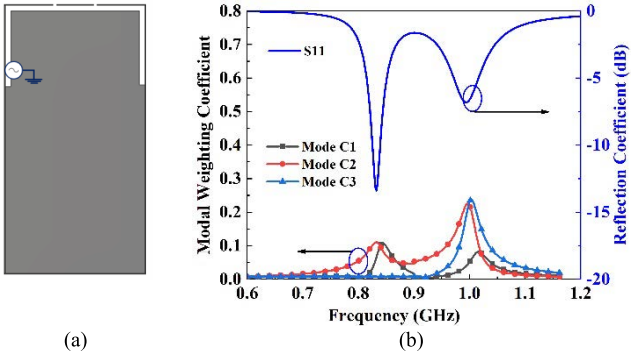

FIGURE 8. Configuration of the inductive exciter. (b) Magnitudes of MWC and the reflection coefficient after adding the exciter.

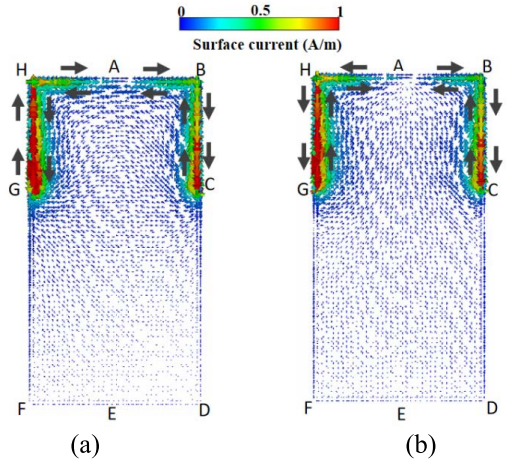

FIGURE 9. Simulated total currents of the open slits configuration. (a) 0.8 GHz. (b) 1.0 GHz.

modes simultaneously, as shown in Fig. 8(a). As depicted in Fig. 8(b), compared to the original structure without open slits, a new resonance is generated at 0.8 GHz. By observing the MWC, we can find that the first resonance at 0.8 GHz is combined by Mode C1 and Mode C2. The second resonance at 1.0 GHz is mainly combined by Mode C2 and Mode C3. Thus, Mode C1 and Mode C2 are excited simultaneously at 0.8 GHz, while Modes C2 and C3 are excited at 1.0 GHz. Clearly, as shown in Fig. 9, the total current distribution and eigencurrents are very similar, which verifies that Modes C1, C2 and C3 are effectively excited. To get good lower bandwidth, we optimized the length of Lb. As shown in Fig. 10, when the feeding source is near grounded point G (at maximum current position), the 6-dB bandwidth can roughly cover the frequency band from 0.82 to 0.98 GHz.

C. EXCITATION AND WORKING PRINCIPLE

Inductive coupling and capacitive coupling are two methods to excite the CMs [29]. The capacitive coupling, called electric excitation in this paper, is located at the minimum current position (maximum electric field position). Inductive coupling, called magnetic excitation in this paper, is always

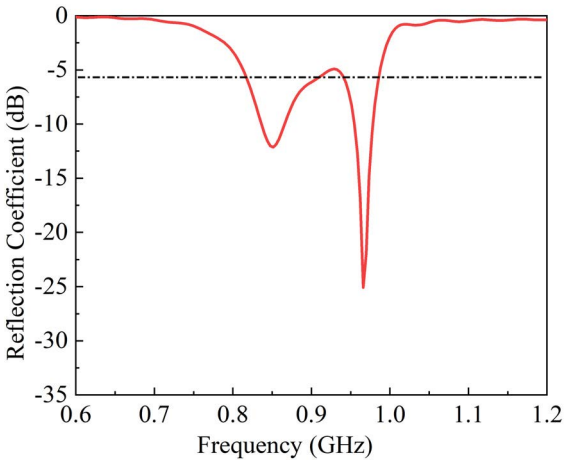

FIGURE 10. Simulated reflection coefficient.

placed at the maximum current position (maximum magnetic field position); electric-magnetic excitation is placed between the maximum and minimum current position; The feeding method mentioned in Section II-B is a magnetic excitation, which can directly feed the metal rim without any matching circuit [2], [3], [6], [17]. When the electric or electric-magnetic feeding method is utilized for metal rim antenna design, an L-shaped feeding line as the excitation is always used to excite the metal rim mode [5], [7], [10], [13], [15], [18]. And it can also be replaced by a capacitor in series with the feeding line, which was used in this paper. The feeding source is located at the corner of the PCB (unlike Section II.B), which divides the U-slot into two parts.

In order to better understand the working principle of the proposed metal rim antenna, the design evolution and simulation working principle of each reference antenna is given in Fig. 11. Ant-1 (feedline without C1), Ant-2 (feedline with C1), Ant-3 (including Ant-2, L2 and a high-pass matching circuit). The simulated reflection coefficients for the above three cases are shown in Fig. 12.

For Ant-1, three resonances are generated at the lower band, the middle band, and the higher band, respectively. Compared to Ant-1, Ant-2 has a new resonant mode generated at the lower band by using a capacitor C1. A new resonant mode at 1.75 GHz can be generated by utilizing an inductor L2, as shown in Fig. 11(c). After using a high-pass matching circuit, the Ant-3 can generate two lower and three higher resonances to cover the lower band (0.82 - 0.96 GHz), the middle band (1.71 - 2.69 GHz), and the higher 5G band (3.4 - 3.8 GHz). Fig. 13 shows the simulated input impedance on the smith chart. It clearly shows the effect of the matching network. This significantly widens the metal rim antenna's lower band bandwidth. The proposed reconfigurable metal antenna, which adds a switch to cover the whole lower band, is introduced in Section II-D.

Fig. 14 shows the simulated current distributions at the corresponding resonant frequencies of 0.93, 1.75, 2.3, and 3.5 GHz in the proposed antenna. Fig.14(a) shows the current

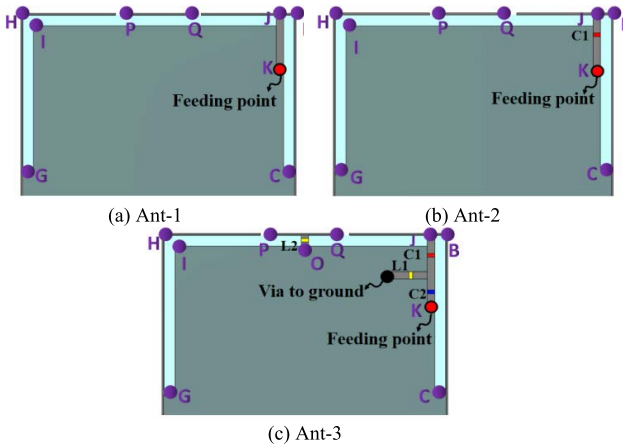

FIGURE 11. Configuration of reference antennas. (L1= 10 nH, L2= 5 nH, C1= 3.3 pF, C2= 1.6 pF).

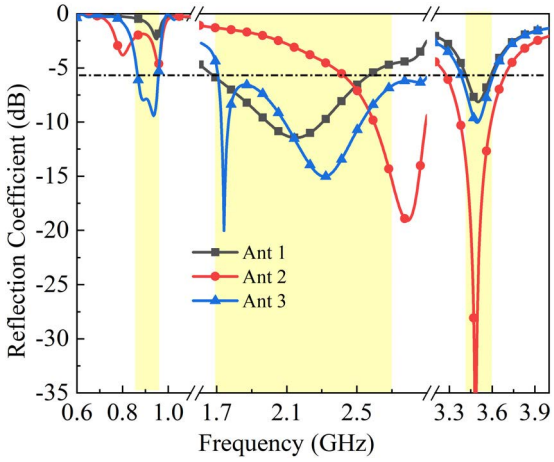

FIGURE 12. Simulated reflection coefficients for Ant-1, Ant-2 and Ant-3.

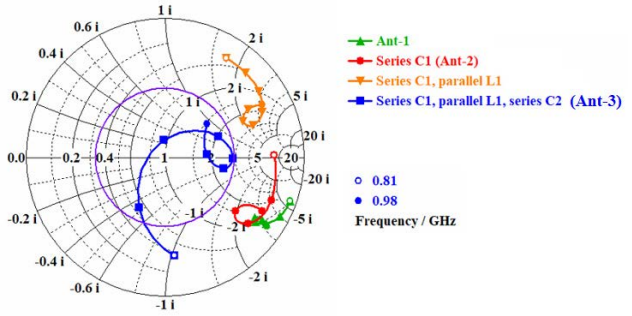

FIGURE 13. Simulated input impedance on the Smith chart for Ant-1 (curve 1), Ant-2 with C1 (curve 2), Ant-2 with C1, L1 and L2 (curve 3), and Ant-3 (curve 4).

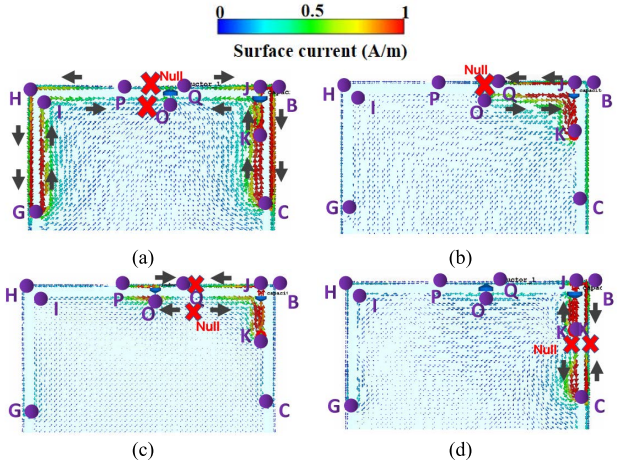

FIGURE 14. Current distributions of the proposed antenna at (a) 0.93 GHz, (b) 1.75 GHz (c) 2.3 GHz (d) 3.5 GHz.

distribution along the U-shaped slot path. It is clearly seen that the current along the path has two nulls, which means the resonant mode at 0.93 GHz is a 1λ loop mode. Fig. 14(b) and (c) show the current distribution along the path JQOKJ. As analyzed in Section II-B, the path JQOKJ can be seen as a small open slot. The resonant modes at 1.75 and 2.3 GHz are slot mode (0.5λ) and open slot mode (1λ), respectively. Fig. 14(d) shows the current mainly distributes in the right metal loop JBCKJ, which generates a 1λ loop resonant mode at 3.5 GHz. Based on the above analysis, we can get the following conclusions. The proposed metal rim antenna works at 1λ loop mode in the lower band. The matching circuit works on the lower band to widen the bandwidth. In the middle and higher band, the slot, open slot, and loop mode are excited.

It is necessary to understand how the design parameters affect antenna performance. To optimize the antenna performance, some important design parameters and their effects are to be studied. Fig. 15(a) shows the effect of changing the length of La. As the length of La (the right shorting end distance) is reduced, the lower band is almost unchanged, and the 5G higher band is shifted down. There is no significant change in the middle band. Similarly, when the length of Lb (the left shorting end distance) decreases, the middle and higher bands keep stable, while the lower band is shifted up. Another important parameter is the location of the inductor L2. As shown in Fig. 15(c), it has a big effect on the middle band. When the length of OQ increases, the resonant modes are all affected. As the value of L2 increases, the lower and higher bands keep stable, and only the second resonance shifts down.

D. INCREASING THE BANDWIDTH FOR THE LOWER BAND

It is not easy to cover the whole lower band (0.69-0.96 GHz) only using a part of the metal rim in a limited antenna clearance of 1 mm. Therefore, the SP4T switch is introduced in the design. The introduction of the SP4T switchwill make it possible to tune the lower band resonant frequency by varying the different channels.

The QPC8013Q used is a low loss and high isolation SP4T switch with performance optimized for LTE and diversity applications. It has four R.F. channels, RF1-RF4. Each channel has a capacitor in series with values of 0.4 pF (RF1),

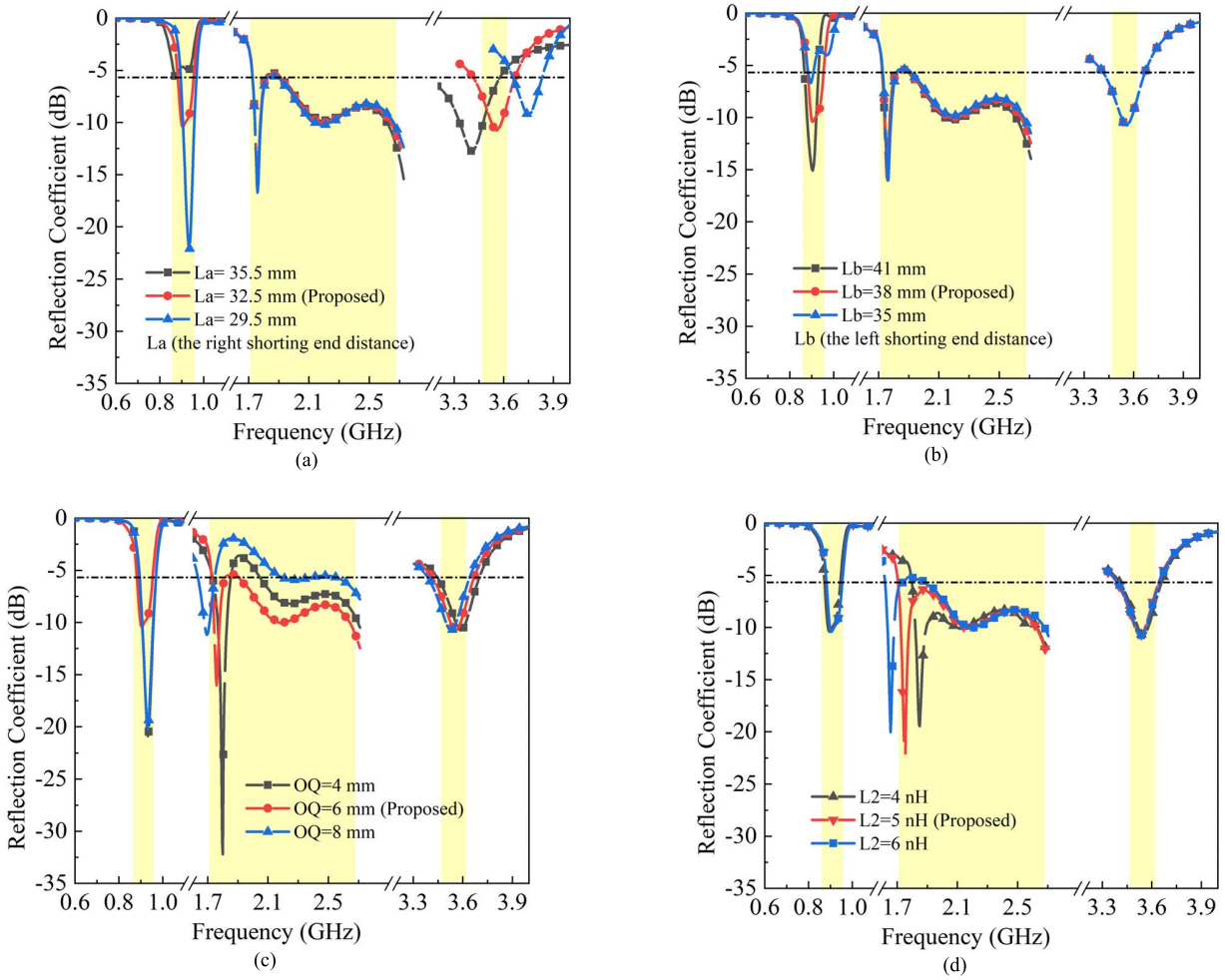

FIGURE 15. Effects of different parameters. (a) Length of La. (b) Length of Lb. (c) Location of inductor L2. (d) The value of L2.

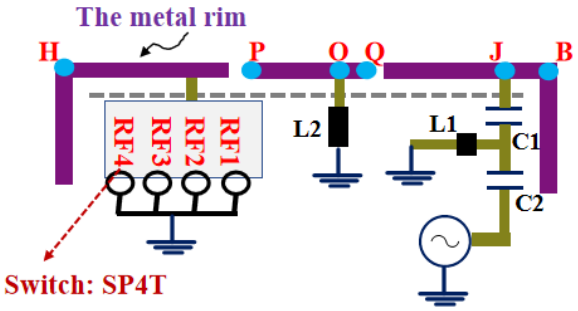

FIGURE 16. The configuration of the SP4T switch.

TABLE 1. Working frequency at different states.

Working state	Channel ON/OFF	Working frequency
State 1	RF 1 ON	0.88-0.96 GHz 1.69-2.69 GHz 3.45-3.70 GHz
State 2	RF 2 ON	0.80-0.88 GHz 1.69-2.69 GHz 3.45-3.70 GHz
State 3	RF 3 ON	0.73-0.80 GHz 1.69-2.69 GHz 3.45-3.70 GHz
State 4	R.F. 4 ON	0.68-0.73 GHz 1.69-2.69 GHz 3.45-3.70 GHz

0.6 pF (RF2), 0.8 pF (RF3), and 1.0 pF (RF4), as shown in Fig. 16. The on/off state of each R.F. channel can be controlled independently.

As shown in Fig. 17(a), the lower frequency bands are shifting by updating the ON/OFF states of the switch, which can enable the proposed antenna to cover 0.69-0.96 GHz. Table 1 summarizes the obtained working frequency band of the proposed antenna with different states. The simulated total efficiency is over 68%, as shown in Fig.17(b).

III. PERFORMANCE EVALUATION

A. FREE SPACE

The proposed reconfigurable metal rim antenna with small clearance is fabricated and measured. As depicted in Fig. 18,

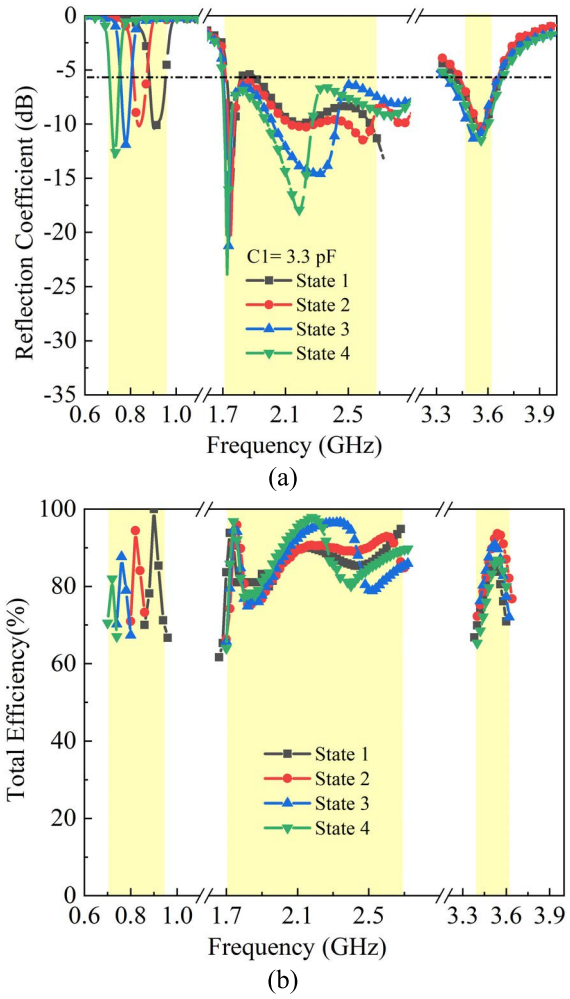

FIGURE 17. Simulated results of proposed antenna for different states when C1=3.3 pF. (a) The reflection coefficients. (b) The total efficiency.

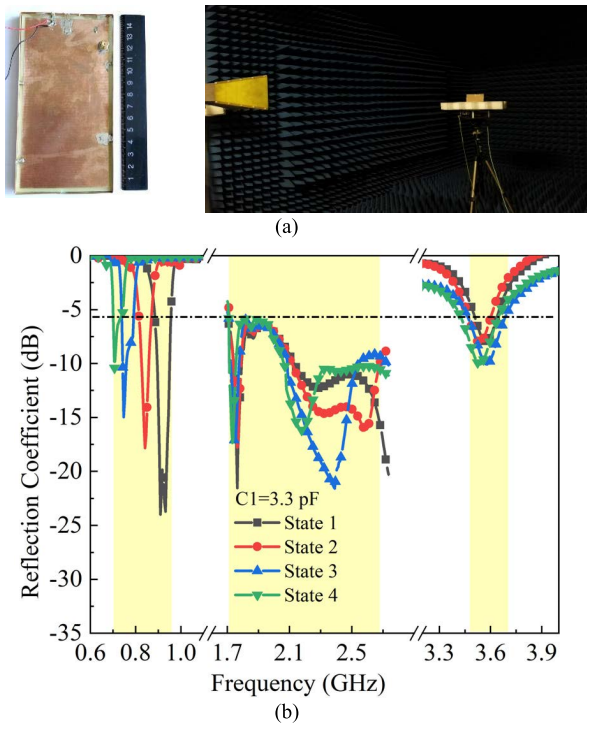

FIGURE 18. (a) Prototype of the proposed metal rim antenna and the measurement setup. (b) Measured reflection coefficient results of the proposed metal rim antenna at different states.

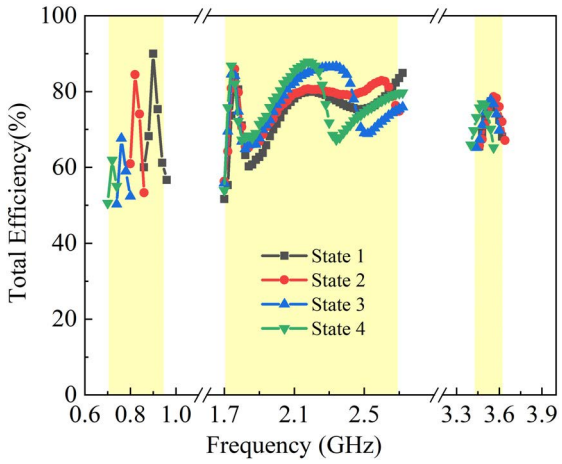

FIGURE 19. Measured total efficiency results of the proposed metal rim antenna at different states.

by changing the channels, the measured 6-dB bandwidths are 270 MHz (0.69-0.96 GHz), 1.2 GHz (1.7-2.9 GHz) and 0.4 GHz (3.4-3.8 GHz), which meets the 4G and 5G frequency band requirements. Furthermore, the measured results are well-validated with the simulated ones, as shown in Figs. 18 and 19. The differences between the measurement and simulation ones are mainly due to fabrication tolerance. As shown in Fig. 19, the measured total efficiency is over 50% for 4G and 5G bands.

As shown in Fig. 20, the simulated and measured normalized radiation patterns in the three principal planes are in good agreement. For the lower band, the radiation pattern is near-omnidirectional. For the high-order resonant frequencies (2.1 and 3.5 GHz), patterns with stronger radiation and more nulls are observed.

B. EFFECTS OF HAND

Fig. 21 shows three different positions when holding the metal rim, namely the top, middle and bottom positions to represent the user's typical hand behaviours. The relative permittivity and conductivity of the human hand model vary with frequency, which has been given in [30]. Generally, the hand of users reduces the total antenna efficiency. The total efficiency of the hand model is shown in Fig. 22. When the user's hand is close to the metal rim antenna, efficiency drops dramatically as expected. The main reason is that the human hand is a lossy medium. It absorbs a considerable part of the radiated power, leading to a low Q-factor. This can be verified by observing the efficiency.

TABLE 2. Comparison between the proposed antennas and references.

Ref.	Utilization of metal rim	Ground clearance (mm)	4G band (MHz)	5G band (MHz)	Total efficiency (%)
[4]	Entire metal rim	2	820-960 1710-2690	3400-3600	4G band: 40-90 5G band: 60-75
[11]	Part of the metal rim	8	824-960 1710-2690	-	4G band: 49-78 -
[15]	Part of the metal rim	10	824-960 1710-2690	-	4G band: 49-76 -
[16]	Entire metal rim	8	824-960 1710-2690	-	4G band: 50-86 -
[17]	Part of the metal rim	15	824-960 1710-2690	-	4G band: 45-80 -
[18]	Part of the metal rim	10	824-960 1710-2690	-	4G band: 42-71 -
[25]	Entire metal rim	11	704-940 1700-2800	-	4G band: 43-76
Prop.	**Part of the metal rim**	**1.0**	**698-960 1710-2900**	**3400-3800**	**4G band: 50-91 5G band: 66-80**

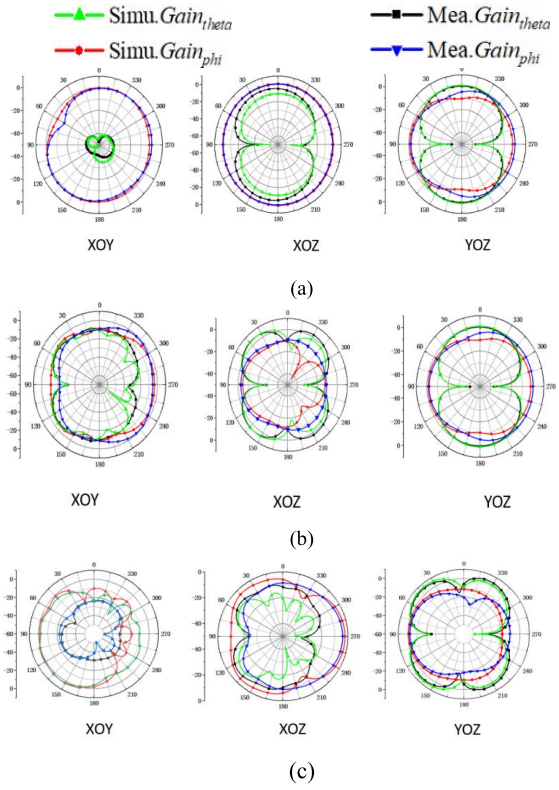

FIGURE 20. Simulated and measured 2-D radiation patterns of the proposed antenna. (a) 0.9 GHz. (b) 2.3 GHz. (c) 3.5 GHz.

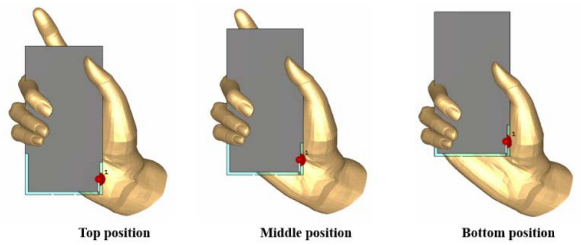

FIGURE 21. Configuration of hand-grip smartphone at different positions.

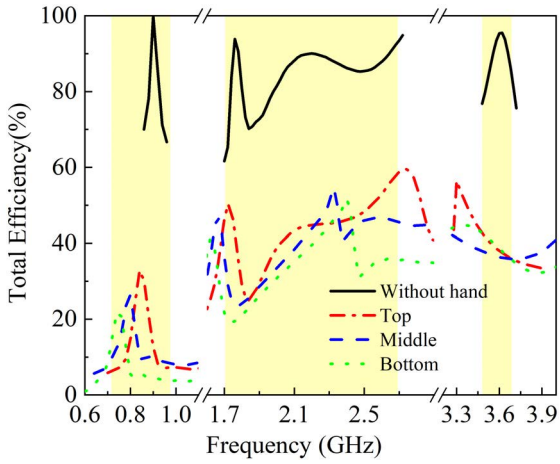

FIGURE 22. The simulated efficiency of hand grip at different positions when C1 = 3.3 pF at state 1.

C. COMPARISON

In order to evaluate the performance of the proposed antenna with respect to available designs, the proposed antenna is compared with recently published designs, as shown in Table 2. The key parameters are the utilization rate of the metal rim, the width of ground clearance, bandwidth, the lower band, the 5G band, and total efficiencies in multiple bands. From Table 1, we can find that the antenna proposed in [4] is suitable for the metal frame and self-decoupled system, but the LTE700 band is not covered. Besides, some antenna systems are not suitable for full-screen metal-frame smartphones because of the large ground clearance. The proposed antenna not only has the ability to cover the 2G/3G/4G bands

but can also meet the sub-6 GHz spectrum of the 5G band. Furthermore, the proposed antenna has a compact, simple structure and does not need large ground

clearance. The limitation of this design needs to use some lump elements and a switch to cover the whole frequency band, which affects the efficiency. However, it still meets the requirement of the full-screen 5G smartphone antenna design.

IV. CONCLUSION

In this paper, a reconfigurable metal rim antenna with the smallest clearance of 1 mm for 4G/5G smartphone applications has been proposed, fabricated, and measured. The proposed antenna was developed through a comprehensive study of TCM and is optimized for the best performance with the smallest clearance and compact size. The metal rim modes with an inductive coupling excitation have been excited. A SP4T switch has been employed to cover the lower band from 0.69 to 0.96 GHz. By employing these arrangements, as demonstrated by the simulation and measurement results, the proposed antenna can cover not only 2G/3G/4G bands (including LTE700, GSM850, GSM 900, DCS, PCS, UMTS2100, LTE2300, and LTE2500) but also 5G bands (3.4- 3.8 GHz). Therefore, the proposed metal rim antenna design is a very good candidate for 5G smartphones and mobile devices.

REFERENCES

[1] Z. Ying, "Antennas in cellular phones for mobile communications," *Proc. IEEE*, vol. 100, no. 7, pp. 2286–2296, Jul. 2012.

[2] R. S. Aziz, A. K. Arya, and S. O. Park, "Multiband full-metal-rimmed antenna design for smartphones," *IEEE Antennas Wireless Propag. Lett.*, vol. 15, pp. 1987–1990, 2016.

[3] Y. L. Ban, Y. F. Qiang, Z. Chen, K. Kang, and J. H. Guo, "A dual-loop antenna design for hepta-band WWAN/LTE metal-rimmed smartphone applications," *IEEE Trans. Antennas Propag.*, vol. 63, no. 1, pp. 48–58, Jan. 2015.

[4] Q. Chen, H. Lin, J. Wang, L. Ge, Y. Li, and T. Pei, "Single ring slot-based antennas for metal-rimmed 4G/5G smartphones," *IEEE Trans. Antennas Propag.*, vol. 67, no. 3, pp. 1476–1487, Mar. 2019.

[5] C. Deng, Z. Feng, and S. V. Hum, "MIMO mobile handset antenna merging characteristic modes for increased bandwidth," *IEEE Trans. Antennas Propag.*, vol. 64, no. 7, pp. 2660–2667, Jul. 2016.

[6] C. Deng, Z. Xu, A. Ren, and S. V. Hum, "TCM-based bezel antenna design with small ground clearance for mobile terminals," *IEEE Trans. Antennas Propag.*, vol. 67, no. 2, pp. 745–754, Feb. 2019.

[7] J.-W. Lian, Y.-L. Ban, Y.-L. Yang, L.-W. Zhang, C.-Y.-D. Sim, and K. Kang, "Hybrid multi-mode narrow-frame antenna for WWAN/LTE metal-rimmed smartphone applications," *IEEE Access*, vol. 4, pp. 3991–3998, 2016.

[8] J. Choi, W. Hwang, C. You, B. Jung, and W. Hong, "Four-element reconfigurable coupled loop MIMO antenna featuring LTE full-band operation for metallic-rimmed smartphone," *IEEE Trans. Antennas Propag.*, vol. 67, no. 1, pp. 99–107, Jan. 2019.

[9] Y. Liu, W. Cui, Y. Jia, and A. Ren, "Hepta-band metal-frame antenna for LTE/WWAN full-screen smartphone," *IEEE Antennas Wireless Propag. Lett.*, vol. 19, no. 7, pp. 1241–1245, Jul. 2020.

[10] Y. Liu, J. Zhang, A. Ren, H. Wang, and C.-Y.-D. Sim, "TCM-based hepta-band antenna with small clearance for metal-rimmed mobile phone applications," *IEEE Antennas Wireless Propag. Lett.*, vol. 18, no. 4, pp. 717–721, Apr. 2019.

[11] Y. Liu, Y.-M. Zhou, G.-F. Liu, and S.-X. Gong, "Heptaband inverted-F antenna for metal-rimmed mobile phone applications," *IEEE Antennas Wireless Propag. Lett.*, vol. 15, pp. 996–999, 2016.

[12] Y. Wang and Z. Du, "Wideband monopole antenna with less nonground portion for octa-band WWAN/LTE mobile phones," *IEEE Trans. Antennas Propag.*, vol. 64, no. 1, pp. 383–388, Jan. 2016.

[13] M. H. Alshamaileh, S. S. Alja'afreh, and E. Almajali, "Nona-band, hybrid antenna for metal-rimmed smartphone applications," *IET Microw., Antennas Propag.*, vol. 13, pp. 2439–2448, Nov. 2019.

[14] Z.-Q. Xu, Y. Sun, Q.-Q. Zhou, Y.-L. Ban, Y.-X. Li, and S. S. Ang, "Reconfigurable MIMO antenna for integrated-metal-rimmed smartphone applications," *IEEE Access*, vol. 5, pp. 21223–21228, 2017.

[15] Z.-Q. Xu, Q.-Q. Zhou, Y.-L. Ban, and S. A. Simon, "Hepta-band coupled-fed loop antenna for LTE/WWAN unbroken metal-rimmed smartphone applications," *IEEE Antennas Wireless Propag. Lett.*, vol. 17, no. 2, pp. 311–314, Feb. 2018.

[16] Y. Yang, Z. Zhao, W. Yang, Z. Nie, and Q.-H. Liu, "Compact multimode monopole antenna for metal-rimmed mobile phones," *IEEE Trans. Antennas Propag.*, vol. 65, no. 5, pp. 2297–2304, May 2017.

[17] H.-B. Zhang, Y.-L. Ban, Y.-F. Qiang, J. Guo, and Z.-F. Yu, "Reconfigurable loop antenna with two parasitic grounded strips for WWAN/LTE unbroken-metal-rimmed smartphones," *IEEE Access*, vol. 5, pp. 4853–4858, 2017.

[18] L.-W. Zhang, Y.-L. Ban, C.-Y.-D. Sim, J. Guo, and Z.-F. Yu, "Parallel dual-loop antenna for WWAN/LTE metal-rimmed smartphone," *IEEE Trans. Antennas Propag.*, vol. 66, no. 3, pp. 1217–1226, Mar. 2018.

[19] D. Huang, Z. Du, and Y. Wang, "A quad-antenna system for 4G/5G/GPS metal frame mobile phones," *IEEE Antennas Wireless Propag. Lett.*, vol. 18, no. 8, pp. 1586–1590, Aug. 2019.

[20] R. Harrington and J. Mautz, "Theory of characteristic modes for conducting bodies," *IEEE Trans. Antennas Propag.*, vol. AP-19, no. 5, pp. 622–628, Sep. 1971.

[21] R. Harrington and J. Mautz, "Computation of characteristic modes for conducting bodies," *IEEE Trans. Antennas Propag.*, vol. AP-19, no. 5, pp. 629–639, Sep. 1971.

[22] J. Dong, S. Wang, and J. Mo, "Design of a twelve-port MIMO antenna system for multi-mode 4G/5G smartphone applications based on characteristic mode analysis," *IEEE Access*, vol. 8, pp. 90751–90759, 2020.

[23] R. Martens, J. Holopainen, E. Safin, J. Ilvonen, and D. Manteuffel, "Optimal dual-antenna design in a small terminal multiantenna system," *IEEE Antennas Wireless Propag. Lett.*, vol. 12, pp. 1700–1703, 2013.

[24] Z. Miers, H. Li, and B. K. Lau, "Design of bandwidth-enhanced and multiband MIMO antennas using characteristic modes," *IEEE Antennas Wireless Propag. Lett.*, vol. 12, pp. 1696–1699, 2013.

[25] P. Qiu and Q. Feng, "Low-profile compact antenna for octa-band metal-rimmed mobile phone applications," *IEEE Trans. Antennas Propag.*, vol. 68, no. 1, pp. 54–61, Jan. 2020.

[26] L. Chen, Y. Huang, H. Wang, and H. Zhou, "Low-frequency band metal rim antenna design using TCM for smartphone application," in *Proc. 13th U.K.-Eur.-China Workshop Millimetres-Waves THz Technol. (UCMMT)*, 2020, pp. 1–3.

[27] L. Chen, Y. Huang, H. Wang, and H. Zhou, "Metal rim antenna with small clearance based on TCM for smartphone applications," in *Proc. 15th Eur. Conf. Antennas Propag. (EuCAP)*, 2021, pp. 1–3.

[28] Y. Chen and C.-F. Wang, *Characteristic Modes: Theory and Applications in Antenna Engineering*. Hoboken, NJ, USA: Wiley, 2015.

[29] R. Martens, E. Safin, and D. Manteuffel, "Inductive and capacitive excitation of the characteristic modes of small terminals," in *Proc. Loughborough Antennas Propag. Conf.*, 2011, pp. 1–4.

[30] C. Gabriel, "Tissue equivalent material for hand phantoms," *Phys. Med. Biol.*, vol. 52, no. 14, pp. 4205–4210, Jul. 2007.

LYUWEI CHEN received the B.S. degree in electronic sciences and technology from the Jilin Agricultural University, Jilin, China, in 2014, and the M.S. degree in electromagnetic field and electromagnetic wave from Huaqiao University, Xiamen, in 2017. He is currently pursuing the Ph.D. degree in mobile terminal devices antennas with the University of Liverpool, Liverpool, U.K.

He was an Antenna and Microwave Engineer with the Shanghai Amphenol Airwave Communication Electronics Company Ltd., Shanghai, China. His research interests include metamaterials and millimeter wave array antennas, mobile phone antenna design, the theory of characteristic modes, and MIMO and mm-wave antenna array design for 5G smartphones.

YI HUANG (Fellow, IEEE) received the B.Sc. degree in physics from Wuhan, China, in 1984, the M.Sc. (Eng.) degree in microwave engineering from Nanjing, China, in 1987, and the D.Phil. degree in communications from the University of Oxford, U.K., in 1994.

He has been conducting research in the areas of antennas, radio communications, applied electromagnetics, radar, and EMC, since 1987. More recently, he is focused on mobile antennas, wireless energy harvesting, and power transfer. His experience includes three years spent with NRIET, China, as a Radar Engineer and various periods with the Universities of Birmingham, Oxford, and Essex, U.K., as a member of Research Staff. He worked as a Research Fellow with British Telecom Laboratories, in 1994, and then joined at the Department of Electrical Engineering and Electronics, University of Liverpool, U.K., as a Faculty Member, in 1995, where he is currently a Full Professor of wireless engineering and the Head of High Frequency Engineering Group and the Deputy Head of Department. He has published over 500 refereed papers in leading international journals and conference proceedings and authored four books, including *Antennas: From Theory to Practice* (John Wiley, 2008, 2021). He has received many patents, research grants from research councils, government agencies, charities, E.U., and industry.

Prof. Huang is a fellow of IET. He was a recipient of over ten awards, such as the BAE Systems Chairman's Award 2017, IET, and the Best Paper Awards. He has served for a number of national and international technical committees and is an editor, an associate editor, or the guest editor of five international journals. In addition, he has been a Keynote/Invited Speaker and an Organizer of many conferences and workshops, such as IEEE iWAT2010, LAPC2012, and EuCAP2018. He is the Editor-in-Chief of *Wireless Engineering and Technology*, an Associate Editor of IEEE Antennas and Wireless Propagation Letters, U.K., and Ireland Rep to European Association of Antennas and Propagation (EurAAP), from 2016 to 2020.

HANYANG WANG (Fellow, IEEE) received the Ph.D. degree from Heriot-Watt University, Edinburgh, U.K., in 1995.

From 1986 to 1991, he served as a Lecturer and an Associate Professor at Shandong University, Jinan, China. From 1995 to 1999, he was a Postdoctoral Research Fellow at the University of Birmingham, Birmingham, U.K., and the University of Essex, Colchester, U.K. From 1999 to 2000, he was at Vector Fields Ltd., Oxford, U.K., as a Software Development and Microwave and an Antenna Engineering Consultant Engineer. He joined at Nokia U.K. Ltd., Farnborough, U.K., in 2001, where he had been a Mobile Antenna Specialist for 11 years. After he joined at Huawei. He is currently the Chief Scientist of mobile terminal antennas and the Head of the Mobile Antenna Technology Division, Huawei Technologies. He leads a large group of antenna experts and engineers and takes the full leadership and responsibility in the research and development of antenna technologies to guarantee the market success of all Huawei's mobile terminal products ranging from smartphones, laptops, tablets, MiFi, data cards, smart watches, BT headsets, routers, the IoT, smart screens, CPE, VR, automobiles, etc. He is also an Adjunct Professor with Nanjing University, Nanjing, China, and Sichuan University, Chengdu, China. He has authored over refereed 120 articles on these topics. He holds over 50 granted US/EU/JP/CN patents, including 31 U.S. patents, and has other 60+ patent applications in pending. His current research interests include small, wideband and multiband antennas for mobile terminals, MIMO antennas and antenna arrays for 5G sub-6GHz, and 5G millimetre wave mobile communications. He is a Huawei Fellow and an IET Fellow. He was a recipient of the Title of Nokia Inventor of the Year, in 2005, the Nokia Excellence Award, in 2011, the Huawei Individual Gold Medal Award, in 2012, and the Huawei Team Gold Medal Award, in 2013 and 2014. His patent was ranked number one among the 2015 Huawei Top Ten Patent Awards. He was an Associate Editor of the IEEE Antennas and Wireless Propagation Letters, from 2015 to 2021.

HAI ZHOU received the Ph.D. degree from the University of London, London, U.K., in 1987.

He was a Postdoctoral Researcher at the University of London, until 1992. He was a Senior Lecturer at South Bank University, London. He joined at Lucent Technologies, in 1996, where he has been involved in system engineering for 19 years. He joined at Huawei Technologies, in 2015, where he is involved in over-the-air test related standards and 5G antennas. He has authored 14 journal articles and 34 conference papers and holds 18 patents. His research interests include shaped reflector antenna synthesis, FDTD during his academic years to radio resource management, and adaptive antennas in industry.

Dr. Zhou was a recipient of the Best Paper Award at the 19th European Microwave Conference, in 1989, and the Oliver Lodge Premium from IEE as the Best Paper of the year on Antennas and Propagation, in 1991.

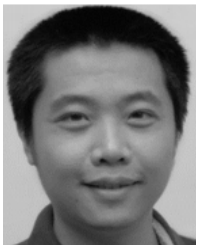

KEXIN LIU was born in Jinan, Shandong, China, in 1988. He received the B.S. degree in optical engineering from Zhejiang University, Hangzhou, Zhejiang, China, in 2011, and the Ph.D. degree in electromagnetic engineering from the KTH Royal Institute of Technology, Stockholm, Sweden, in 2016. He joined at Huawei Technologies, Shanghai, China, in 2016, where he is currently a Senior Expert of mobile phone antenna. His research interests include nonreciprocal propagation of electromagnetic waves, mobile phone antenna design, ultrawideband antenna design, and 5G antenna systems.